Trace detection of canine distemper virus based on Michelson-interferometer sensing probe

Xinyu Zhang[1], Xiangyu Hou[2], Wenlin Feng[1,3*]

[1]*School of Science, Chongqing University of Technology, Chongqing 400054, China.*

[2]*School of Pharmacy and Bioengineering, Chongqing University of Technology, Chongqing 400054, China.*

[3]*Chongqing Key Laboratory of Green Energy Materials Technology and Systems, Chongqing 400054, China.*

Abstract: A single-mode-fiber (SMF)-multimode-fiber (MMF)-tri-core-fiber (TCF) Michelson probe structure is proposed for trace detection of canine distemper virus (CDV). One end of the TCF is cut flat and fused with the multimode fiber, and the other end is coated with a silver film to enhance the reflection, and an optic-fiber sensing probe with SMF-MMF-TCF structure is obtained. The $(PDDA/PSS)_3$ multilayer film is modified on the surface of the fiber by layer-by-layer self-assembly method as a polyelectrolyte binder to immobilize CDV antibodies to form a $(PDDA/PSS)_3$/CDV antibody composite membrane for specific detection of CDV antigens. The response-recovery test of the sensor is performed to verify its repeatability. The detection limit, the sensitivity, and the linear fitting degree for CDV antigen are 0.1236 pg/ml, 1.1776 dB/(pg/ml), and 0.9899, respectively. At the same time, the stability, selectivity, and clinical samples of the sensors were also verified.

Keywords: Optic-fiber biosensor; Michelson interferometer; layer-by-layer self-assembly; canine distemper virus

1. Introduction

Canine distemper (CDV) is a fatal pantropic measles virus in dogs [1]. It has spread worldwide since its discovery in 1760. CDV virus can not only infect puppies, but also parasitize organisms such as Carnivora and Raccoonidae, resulting in diarrhea,

*Corresponding author. Tel.: +86 23 6256 3151. E-mail address: wenlinfeng@126.com (W.L. Feng).

immunocompromise, and thus concurrent bacterial infections and even death [2,3]. The host range of CDV has been extended to non-human primates. A strain of canine distemper virus (CYN07-dV) was detected in Vero cells of cynomolgus signaling lymphocyte activation molecule (SLAM) in 2008 in crab-eating monkeys, suggesting the existence of a persistent chain of CDV infections in the monkey population [4]. Infections in primates have raised concerns about the potential threat of zoonotic diseases [5,6].

Many studies have been conducted on the detection of canine distemper virus. The main detection methods include enzyme-linked immunosorbent assay (ELISA) [7], ring-mediated isothermal amplification reaction [8], polymerase chain reaction (PCR) [9], reverse transcription-polymerase chain reaction (RT-PCR) [10], gene chip technology [11], colloidal gold immunochromatography [12], immunofluorescence [13], and agar diffusion assay [14]. However, the above methods have problems such as complex operation, susceptibility to interference, harsh detection environment, and susceptibility to false positives. Optic-fiber sensors have the advantages of high sensitivity, miniaturization, telemetry, easy operation, and low cost [15-17], among which surface plasmon resonance (SPR) [18,19], surface-enhanced Raman scatting (SERS) [20], coupled micro-ring resonators [21], resonant diffraction grating surfaces [22], and optic-fiber gratings [23] have been used for the detection of biological samples. Guo et al. achieved highly sensitive detection of urinary proteins using a tilted grating optic-fiber sensor with plasma nanocoating with the detection limit of 1.5×10^{-3} mg/ml [24]; Ribaut et al. achieved detection of the cancer biomarker cytokeratin 17 (CK17) by using encapsulated plasma grating optical fiber with the detection limit of 10^{-12} g/ml [25]; Wen et al. achieved the detection of MicroRNA by using a U-shaped optic-fiber with the detection limit of 0.0133 ng/ml [26]. Luo et al. used a graphene oxide cladding double-peaked long-period optical fiber grating for the label-free and specific analysis of the H5N1 virus with a detection limit of 1.05 ng/ml [27]. Therefore, the realization of trace detection of biological samples based on optic-fiber sensing technology has a very great potential application.

In this work, a Michaelson interferometric optic-fiber sensor with SMF-MMF-TCF

structure is proposed, in which layers of poly dimethyl diallyl ammonium chloride (PDDA) and polystyrene sulfonic acid (PSS) are alternately self-assembled on the TCF, and then modified with CDV antibody to achieve specific detection of CDV antigen, and the sensing performance of the sensor is discussed and investigated. Meanwhile, antigen-antibody dissociation experiments are performed on the sensor, the optic-fiber sensor could repeatedly detect CDV antigen. Finally, the testing of clinical samples is performed to verify the practicality of this optic-fiber CDV sensor.

2. Basic principle

The system diagram of the optic-fiber sensor for canine distemper antigen is shown in Fig. 1, which consists of a broad-spectrum light source (ASE), a spectrometer (OSA), and a circulator. The dashed line is the amplification image of the sensing region, which is formed by the SMF-MMF-TCF Michelson interference sensing structure (the core diameters of the SMF, MMF and TCF are 9 μm, 105 μm and 8.6 μm, respectively). $(PDDA/PSS)_3$/CDV antibody composite film is coated on the TCF, which the end is sliced flat and then coated with a silver film. The length of the TCF and MMF is 3 cm and 0.5 cm, respectively. The optic-fiber sensor is connected with the ASE and the OSA through a circulator.

Fiber core mismatch occurs when light is transmitted from SMF to MMF, which excites the higher-order modes. Part of the light enters the TCF core, another part is transmitted in the TCF cladding, and finally reflects at the silver film of the TCF. The reflected light enters the OSA after being converged by the MMF, the two paths of light satisfy the interference conditions and produce an interference spectrum, which is simulated to decrease in intensity with increasing refractive index (see Fig. S1 of Supporting Information). The reflected light intensity of the Michelson interference structure is expressed as [28],

$$I = R^2(n_s)(I_1 + I_2 + 2\sqrt{I_1 I_2}\cos\Delta\varphi) \quad (1)$$

where R is the Fresnel reflection coefficient, n_s is the surrounding refractive index, I_1 and I_2 are the TCF core light intensity and cladding light intensity, respectively, and $\Delta\varphi$

is the phase difference. The phase difference is related to the length of the TCF and the effective refractive index difference between the interference modes, which is defined as [29],

$$\Delta\varphi = \frac{4\pi}{\lambda}\Delta n_{\mathrm{eff}} L \tag{2}$$

where Δn_{eff} is the difference between the effective refractive index of the TCF core and cladding, L is the length of the TCF, and λ is the wavelength of the incident light signal. When $\Delta\varphi=2(m+1)\pi$, the condition of interferential phase cancellation is satisfied, and an interference spectrum is generated. When the specific binding of antigen-antibody on the surface of TCF occurs, the interaction between the functional film and the measured molecules results in a change in the effective refractive index of the cladding mode, which leads to a change in the optical path of the cladding mode. However, the optical path of the core mode remains unchanged, so the optical path difference will change. The concentration of CDV antigen can be determined by monitoring the change in the intensity of the interferometric trough.

3. Experiment

3.1 Materials and Equipment

The reagents required for the experiments are analytically pure, poly dimethyl diallyl ammonium chloride (PDDA, Macklin, China), polystyrene sulfonic acid (PSS, Macklin, China), silver nitrate ($AgNO_3$, Kelon Chemicals, China), ammonia (NH_3, Chuandong Chemicals, China), Potassium hydroxide (KOH, Aladdin, China), glucose ($C_6H_{12}O_6.H_2O$, Aladdin, China), and dry powder of PBS buffer (0.01 M pH=7.2-7.4, Beijing Kulabo, China). Biological samples used in this experiment: canine distemper antibody (sample purity of>90%, the concentration of 100 ng/ml), canine distemper antigen (sample purity of>90%, concentration of 0.1, 1, 10, 50, 100, 1000, 10000 pg/ml), alpha-fetoprotein antigen (AFP), toxoplasma gondii antigen (SAG1), H9N2 antigen (H9N2), bovine serum albumin (BSA), ovalbumin (OVA), and bovine hemoglobin (HGB) are prepared in the laboratory of the School of Pharmacy and Bioengineering, Chongqing Polytechnic University, and the purity of the samples is more than 90%.

Canine distemper-negative clinical samples and canine distemper-positive clinical samples are provided by Chongqing Center for Animal Disease and Preventive Control. The composition of the antibody sealing solution is high protein skimmed high calcium milk powder. The equipment used in this experiment is a dip coater (SYDC-100M, Shanghai ShanYan Co, Ltd., China), ASE light source (C+L band, Kangguan, China), spectral analyzer (AQ6370D, Yokogawa, Japan), and optical fiber fusion splicer (S178C, Furukawa, Japan), constant temperature and humidity incubator (HWS-80B, Wanruigude, China).

3.2 Sensor fabrication

3.2.1 Sensing structure

One end of the TCF is fused to the MMF, and the other end is coated with a silver film through a silver mirror reaction to enhance the reflection and encapsulate with UV adhesive to prevent oxidation. According to Eq. (2), the length of TCF will affect the interference spectrum. The reflectance spectra of different TCF lengths are shown in Fig. 2(a)-(f). When the TCF length is 1 cm and 2 cm, the interference fringes have high contrast and the number of troughs is suitable for observation (Fig. 2(a)-(b)). However, its shorter length reduces the binding sites for canine distemper antigens. When the length is 3 cm, there are a few stable and sharp interference troughs within the range of 1520 nm-1620 nm, it can be used to monitor the change of the interference spectrum, as shown in Fig. 2(c). When the length is 4 cm, 5 cm, or 6 cm, the interference troughs are very dense, the small free spectral area is not suitable to observe the interference trough changes, as shown in Fig. 2(d)-(f). The above experimental results are consistent with the simulation results (see Fig. S2 of Supporting Information), the length of the TCF in the subsequent experiments is 3 cm.

3.2.2 Optimal number of sensing membrane layers

Surface charge is necessary for electrostatic self-assembly and the charge is estimated by zeta potential measurements. The zeta potentials of the PDDA and PSS solutions used in this work are +49.99 mV and -39.02 mV, respectively. Due to the high absolute

zeta potentials of PDDA and PSS, these two polymers have been widely used for layer-by-layer (LBL) self-assembly [30].

To investigate the effect of different numbers of composite film (PDDA/PSS) layers on the sensitivity of the sensor, the experiments were conducted as shown in Fig. S3 (Supporting Information). The reflectance spectra are shifted slightly when the coated number is 1 and 2(see Fig. S3(a)-(b) of Supporting Information). When the number of coating layers is 3 or 4, the interference spectrum changes more obviously (see Fig. S3(c)-(d) of Supporting Information). However, the interference trough near 1550 nm is distorted when the coating number is 4, probably because excessive film layers increase the surface roughness of the fiber, which weakens the reflected light intensity and distorts the waveform. Therefore, the coating number in the subsequent experiments is 3.

3.3 Preparation of sensing materials and construction of sensing system

PDDA is used to prepare a polycationic solution (2 mg/ml, 0.5 M NaCl), and PSS is used to prepare a polyanionic solution (2 mg/ml, 0.5 M NaCl). The solvent is deionized water, and the water did not contain other ionic components to avoid interfering with the polarity of the solution. PBS buffer is used to configure 100 μg/ml canine distemper antibody solution and different concentrations of canine distemper antigen solution (0.1, 1, 10, 50, 100, 1000, 10000 pg/ml).

The process of CDV antibody modification of the fiber surface is shown in Fig. 3. The PDDA polycation solution and PSS polyanion solution were ultrasonicated for 20 min to make them uniformly dispersed. After cleaning the surface with deionized water and ethanol, the optic-fiber sensing probe was firstly immersed in PDDA solution for 8 min, and rinsed with deionized water 3 times to remove free PDDA ions from the surface. Then immersed in the PSS solution and repeated the above process. A PDDA/PSS film is assembled on the TCF surface due to the electrostatic effect. The above process was repeated three times to obtain the optic-fiber sensing probe modified with $(PDDA/PSS)_3$ composite sensing film. Secondly, the optic-fiber sensing probe was immersed in a CDV antibody solution for 1 h, and the CDV antibody-modified fiber

optic sensor was obtained. Thirdly, washed fiber optic sensor with PBS buffer and then immersed in 10% milk powder solution to seal the excess active sites on the fiber surface. The prepared CDV optic-fiber sensor was sequentially immersed in a gradient concentration of CDV antigen solution, and the sensor was rinsed with PBS after each test to remove the antigen molecules free on the surface of the sensor to avoid affecting the next measurement results.

4. Results and discussion

4.1 SEM

The microscopic morphology of the $(PDDA/PSS)_3$ composite film can be obtained by scanning electron microscopy (SEM). Fig. 4(a) shows the morphology of the $(PDDA/PSS)_3$ composite film when it is coated on the surface of the TCF, and after layer-by-layer self-assembly, the $(PDDA/PSS)_3$ composite film was homogeneous and dense. From the fiber cross-section SEM image, the thickness of the multilayer film is about 39.34 nm (shown in Fig. 4(b)).

4.2 AFM

Fig. 5 shows the atomic force microscopy (AFM) images and phase image of the $(PDDA/PSS)_3$ multilayer film. From the Fig. 5(a), the surface roughness of the fiber is around 7.87 nm, and the colors in the phase image are uniform, indicating that the two polymers, PDDA/PSS, have the same adhesion force and the film formation is more uniform. When the surface is modified with CDV antibody, the surface roughness of the optic-fiber is slightly reduced to about 7.05 nm, which may be due to the adsorption of CDV antibody to fill the gap on the surface of $(PDDA/PSS)_3$ composite film (shown in Fig. 5(b)). The corresponding phase image shows two different colors, indicating that the adhesion of the CDV antibody is different from that of the $(PDDA/PSS)_3$ composite membrane. Fig. 5(c) and (d) show the CDV antibody binds to 10 pg/ml and 10 ng/ml CVD antigen, respectively. Due to the formation of biomolecules after antigen-antibody binding, the surface roughness of the fiber increased significantly to 21.1 nm and 23.0 nm, respectively. The color of the phase image is more homogeneous, indicating that

the same substance is adsorbed on the surface of the composite material, and the CDV antigen binds specifically to the antibody.

4.3 Effect of different materials on sensor performance

In order to investigate the effect of different materials on the performance of CDV optic-fiber sensors, two identical SMF-MMF-TCF Michelson (MI) interference optic-fiber probes were fabricated and modified. One is modified with $(PDDA/PSS)_3$/CDV antibody and labeled as "MI1"; the other is modified with $(PDDA/PSS)_3$ and labeled as "MI2". The two optic-fiber sensors were immersed in the same concentration range of CDV antigen solutions to monitor the spectrum changes, and the data were recorded. Fig. 6 shows that the spectral intensity of MI1 varied much more than MI2 in the range of CDV antigen concentration from 0.1 to 10000 pg/ml, which indicates that the variation of the interference spectral intensity is mainly caused by the specific binding of the antigen and antibody. Therefore, the $(PDDA/PSS)_3$/CDV antibody was used as the sensing material for the sensor in the subsequent experiments.

4.4 CDV antigen measurement

The prepared CDV fiber sensing probe was immersed in PBS buffer to record the background spectra, and then sequentially immersed in different concentrations of CDV antigen solutions (0.1, 1, 10, 50, 100, 1000, 10000 pg/ml), and the changes in the interference spectra were recorded until the reflectance spectra stabilized. The optic-fiber sensor was first rinsed three times with PBS buffer to wash away CDV antigen molecules free on the surface of the fiber, and then the optic-fiber sensing probe was immersed in PBS, at which point the spectrum was recorded. As shown in Fig. 7, the intensity of the interference spectrum near 1570 nm decreased with the increasing concentration of CDV antigen, with the maximum intensity change of 5.842 dB, and the trough intensity is fitted linearly with a fitting coefficient of 0.9899. The limit of detection (*LOD*) is calculated by [31],

$$LOD = \frac{3\sigma}{K} \tag{4}$$

where K is the slope of the linear fit (1.1776) and σ is the standard deviation of the slope (0.0485). Based on the above equation, the detection limit of the sensor is calculated to be 0.1236 pg/ml and the sensitivity is 1.1776 dB/(pg/ml).

4.5 Effect of different pH on sensor recovery performance

Repeatability is one of the most important indicators of sensor performance. The elution of CDV antigen from the surface of the fiber is based on the chemical mechanism that low pH can change the distribution of the surface charge of the conjugate so that they carry the same charge and then repel each other until separation. In the HCl buffer system, CDV antigens are more likely to aggregate and precipitate, thus achieving dissociation. Therefore, the effect of HCl buffer solution in the range of pH 1-4 on the recovery performance of the sensor is explored, the results are shown in Fig. S4 of Supporting Information. When the pH value of HCl was 1 and 2, the recoveries were only 6.53% and 5.67%, respectively. It may be due to the high concentration of HCl that causes massive death of CDV antibodies. When dissociation was performed with HCl at pH=3, the recovery rate is higher at 91.04%. When the pH value was 4, due to the low HCl concentration, part of the antigen did not dissociate successfully, and the recovery rate was only 30.67%. Therefore, HCl with pH=3 is chosen as the dissociative agent for the subsequent experiments.

4.6 Response/recovery testing

Five response/recovery tests were performed on the CDV optic-fiber sensor to evaluate its repeatability. The sensor was immersed in 10 ng/ml CDV antigen solution, and the spectrum data were recorded every 5 min until the interference spectrum no longer changed. The sensor response curve is obtained as shown in Fig. 8, with a response time of about 30 min. During the recovery test, the optic-fiber sensing probe was immersed in 0.01 M HCl solution (pH=3) and the data were recorded every 5 min until the spectrum no longer changed. The above adsorption and dissociation processes were repeated five times, and the response/recovery curves of the CDV sensors were obtained. From Fig. 8, the repeatability of the optic-fiber sensors is higher after the

second and third cycles, with 91.04% and 77.9%, respectively. The repeatability decreased after the 4th and 5th cycles, with 63.8% and 48.9%, which may be attributed to the fact that multiple adsorption/dissociation processes lead to a decrease in the activity of the CDV antibody modified on the fiber surface, and the active sites available for specific binding to CDV antigen during adsorption are reduced.

4.7 Selectivity and stability

The optic-fiber sensing probe modified with CDV antibody was immersed into the same concentration of CDV, BSA, AFP, H9N2, HGB, OVA, and SAG1 antigen solutions, respectively. The response spectrum of the sensor was monitored, and the amount of variation in the intensity of the interference spectrum is shown in Fig. 9(a). The intensity changes by the other antigen solutions are less than 20% of the change caused by CDV antigen solution at the same concentration, indicating that the sensor has excellent selectivity to CDV antigen. The sensor was placed in a constant temperature and humidity chamber to test the temperature stability of the sensor in the range of 20-65°C, and the spectrum data were recorded every 5°C. The scatter plot is shown in Fig. 9(b), and the maximum intensity change caused by temperature is only 0.3847 dB, which had a negligible effect on the sensor. Meanwhile, the time stability of the sensor was carried out in a constant temperature and humidity chamber, and the spectrum data were recorded every 15 min (shown in Fig. 9(c)). The sensor is in dynamic equilibrium within 180 min, and the maximum intensity change is 0.2821 dB, indicating that the sensor has good time stability.

Table 1 compares several different methods for the detection of CDV antigen, the CDV optic-fiber sensor proposed in this experiment has a lower detection limit compared to other types of sensors.

4.8 Clinical sample testing

In order to verify the practicality of the sensor, the clinical sample testing is shown in Fig. 10, where samples 1-3 are CDV activity-positive samples and 4-5 are activity-negative samples. The maximum change in the intensity of the interference spectrum

caused by the positive samples is 3.4353 dB, while the negative sample is only 0.4327 dB, which is less than 20% of the change in light intensity caused by the positive samples, indicating that it can be realized the detection of the clinical samples of canine distemper antigen.

5. Conclusions

In summary, a Michelson interferometric optic-fiber sensor with SMF-MMF-TCF structure was designed to achieve trace detection of CDV antigen by the LBL self-assembly method. Using a polyelectrolyte self-assembled multilayer membrane constructed from PDDA and PSS as a binding agent for CDV antibody modification onto the surface of the fiber. The CDV antibody is successfully modified onto the multilayer membrane. Two identical MI optic-fiber sensors were modified separately, one group was modified with $(PDDA/PSS)_3$/CDV antibody, and the other group was unmodified with CDV antibody solution, the test results show that the response of the sensors is mainly caused by the specific binding of the antigen-antibody. The sensor has a detection limit of 0.1236 pg/ml and a sensitivity of 1.1776 dB/(pg/ml) with a fit coefficient of 0.9899 for CDV antigen solutions. A repeatability test of the sensor was carried out and the sensor repeatability is 91.04% and 77.9% after the second and third cycles, respectively. At the same time, the sensor has excellent selectivity, good temperature, and time stability. At present, the study of optic-fiber CDV sensors based on Michelson interferometric has not been reported, and the CDV optic-fiber sensor proposed in this work has the advantages of high sensitivity, good selectivity, and low detection limit, which has a good application prospect in the field of CDV specific detection.

Declaration of Competing Interest

The authors declare that they have no known competing financial interests or personal relationships that could have appeared to influence the work reported in this paper.

Acknowledgments

The authors would like to acknowledge support from the National Natural Science Foundation of China (51574054), Chongqing Municipal Education Commission (KJZD-K202201107), Chongqing Science and Technology Bureau (cstc2021jcyj-msxmX0493, CSTB2022NSCQ-MSX0356), Joint Fund of Chongqing Municipal Education Commission and Science and Technology Bureau (CSTB2022NSCQ-LZX0032). Chongqing University of Technology (gzlcx20223283).

ORCID iD

Wenlin Feng https://orcid.org/0000-0003-4710-3640

References

[1] A. Beineke, W. Baumgärtner, P. Wohlsein, *ONE HEALTH-AMSTERDAM*. **2015**, 1, 49.

[2] J. Duque-Valencia, N. Sarute, X. A. Olarte-Castillo, J. Ruíz-Sáenz, *Viruses*. **2019**, 11, 582.

[3] J. Zhao, Y. Ren, *Viruses*. **2022**, 14, 1520.

[4] K. Sakai, N. Nagata, Y. Ami, F. Seki, Y. Suzaki, N. L.wata-Yoshikawa, T. Suzuki, *J. Virol.* **2013**, 87, 1105.

[5] L. Alves, M. Khosravi, M. Avila, N. Ader-Ebert, F. Bringolf, A. Zurbriggen, M. Vandevelde, P. Plattet, *J. Virol.* **2015**, 89, 5724.

[6] M. Martinez-Gutierrez, J. Ruiz-Saenz, *BMC Vet. Res.* **2016**, 12, 1.

[7] D. S. Y. Ong, S. J. de Man, F. A. Lindeboom, J.G.M Koeleman, *Clin. Microbiol. Infect.* **2020**, 26, 1094. e7.

[8] M. Chaouch, *Rev. Med. Virol.* **2021**, 31, e2215.

[9] T. E. Miller, W. F. G. Beltran, A. Z. Bard, T. Gogakos, M. N. Anahtar, M. G. Astudillo, D. Yang, J. Thierauf, A. S. Fisch, G. K. Mahowald, M. J. Fitzpatrick, V. Nardi, J. Feldman, B. M. Hauser, T. M. Caradonna, H. D. Marble, L. L. Ritterhouse, S. E. Turbett, J. Batten, N. Z. Georgantas, G. Alter, A. G. Schmidt, J. B. Harris, J.A. Gelfand, M. C. Poznansky, B. E. Bernstein, D. N. Louis, A. Dighe, R. C. Charles, E. T. Ryan, J. A. Branda, V. M. Pierce, M. R. Murali, A. J. Iafrate, E. S. Rosenberg, J. K. Lennerz, *FASEB J.* **2020**, 34, 13877.

[10] A. Tahamtan, A. Ardebili, *Expert Rev. Mol. Diagn.* **2020**, 20, 453.

[11] S. J. Hachey, C. C. W. Hughes, *Lab Chip*. **2018**, 18, 2893.

[12] Y. Wu, M. Wu, C. Liu, Y. Tian, S. Fang, H. Yang, B. Li, Q. Liu, *Food Control*. **2021**, 126, 108052.

[13] W. C. C. Tan, S. N. Nerurkar, H. Y. Cai, D. Wu, Y. T. F. Wee, J. C. T. Lim, *Cancer Commun.* **2020**, 40, 135.

[14] M. Meerwein, A. Tarnutzer, M. Böni, F. V. Bambeke, M. Hombach, A. S. Zinkernagel, *Antibiotics*. **2020**, 9, 218.

[15] T. Y. Liu, Y. B. Wei, G. B. Song, B. X. Hu, L. Q. Li, G. Xian, *Measurement.* **2018**, 124, 211.

[16] M. Nascimento, M. S. Ferreira, J. L. Pinto, *Measurement.* **2017**, 111, 260.

[17] R. Min, Z. Liu, L. Pereira, C. Yang, Q. Sui, C. Marques, *Opt Laser Technol.* **2021**, 140, 107082.

[18] Y. Zhao, R. Tong, F. Xia, Y. Peng, *Biosens. Bioelectron.* **2019**, 142, 111505.

[19] S. Lepinay, A. Staff, A. Ianoul, J. Albert, *Biosens. Bioelectron.* **2014**, 52, 337.

[20] C. B. Adamo, A. S. Junger, L. P. Bressan, J. A. Fracassi Silva, R. J. Poppi, L. Pereira Jesus, *Microchem. J.* **2020**, 156, 104985.

[21] K. W. Kim, J. Song, J. S. Kee, Q. Liu, G. Q. Lo, M. K. Park, *Biosens. Bioelectron.* **2013**, 46, 15.

[22] H. Yan, L. Huang, X. Xu, S. Chakravarty, N. Tang, H. Tian, R. T. Chen, *Opt. Express*. **2016**, 24, 29724.

[23] H. Y. Wen, S. F. Wang, C. H. Li, Y. T. Yeh, C. C. Chiang, *Anal. Chem.* **2020**, 92, 15989.

[24] T. Guo, F. Liu, X. Liang, X. Qiu, Y. Huang, C. Xie, P. Xu, J. Albert, *Biosens. Bioelectron.* **2016**, 78, 221.

[25] C. Ribaut, M. Loyez, J. C. Larrieu, S. Chevineau, P. Lambert, M. Remmelink, R. Wattiez, C. Caucheteur, *Biosens. Bioelectron.* **2017**, 92, 449.

[26] H. Y. Wen, C. W. Huang, Y. L. Li, J. L. Chen, Y. T. Yeh, C. C. Chiang, *Sensors.* **2020**, 20, 1509.

[27] B. Luo, Z. Liu, X. Wang, S. Shi, N. Zhong, P. Ma, S. Wu, *J Biophotonics.* **2021**, 14, e202000279.

[28] H. Lu, X. Wang, S. Zhang, F. Wang, Y. Liu, *Opt Laser Technol.* **2018**, 101, 507.

[29] B. Wang, K. Ni, P. Wang, Q. Ma, W. Tian, L. Tan, *Opt. Fiber Technol.* **2018**, 46,302.

[30] Y. S. Joung, C. R. Buie, *ACS Appl. Mater. Interfaces.* **2015**, 7, 20100.

[31] C. Y. Chiang, T. T. Huang, C. H. Wang, C. J. Huang, T. H. Tsai, S. N. Yu, *Biosens.*

Bioelectron. **2020**, 151, 111871.

[32] Z. Li, Y. Zhang, H. Wang, J. Jin, W. Li, *Can. J. Vet. Res.* **2013**, 77, 303.

[33] C. R. Basso, J. R. Sempionatto, C. C. Tozato, G. C. Rocha, V. A. Pedrosa, *IEEE Sens. J.* **2015**, 15, 4677.

[34] J. Wang, Y. Luo, L. Liang, J. Li, S. Cui, *Arch. Virol.* **2018**, 163, 3345.

[35] T. Mazzu-Nascimento, F. C. Donofrio, B. C. Bianchi, *Braz Arch Biol Technol.* **2018**, 60.

Figures, Captions and Table:

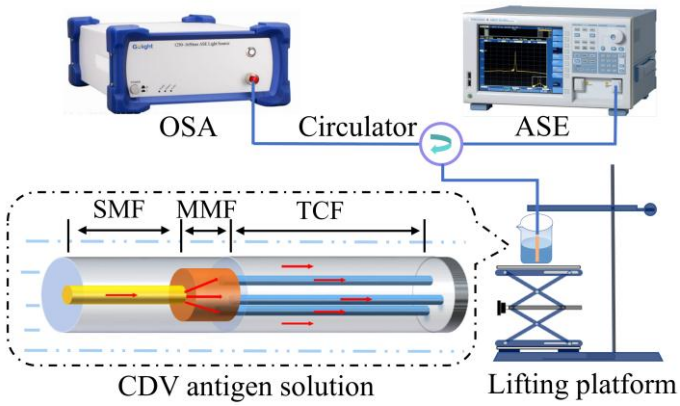

Fig. 1. Optic-fiber sensing system and the inset is sensing region.

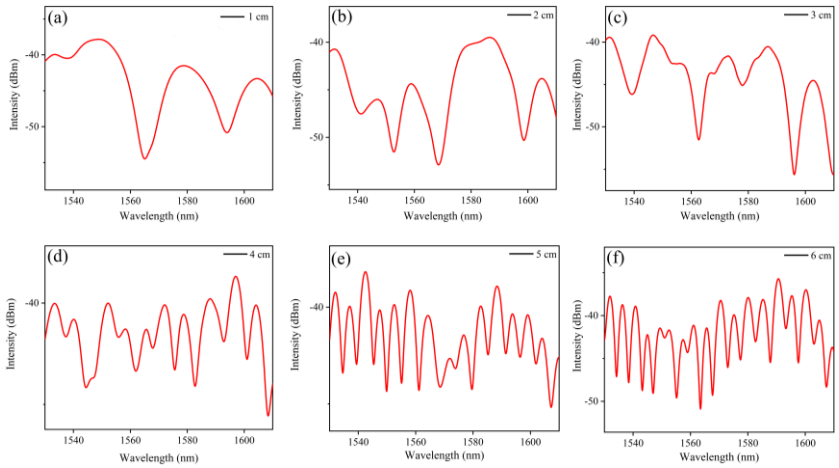

Fig. 2. Sensor reflection spectrum of tri-core fiber with different lengths: (a) 1 cm, (b) 2 cm, (c) 3 cm, (d) 4 cm, (e) 5 cm, and (f) 6 cm.

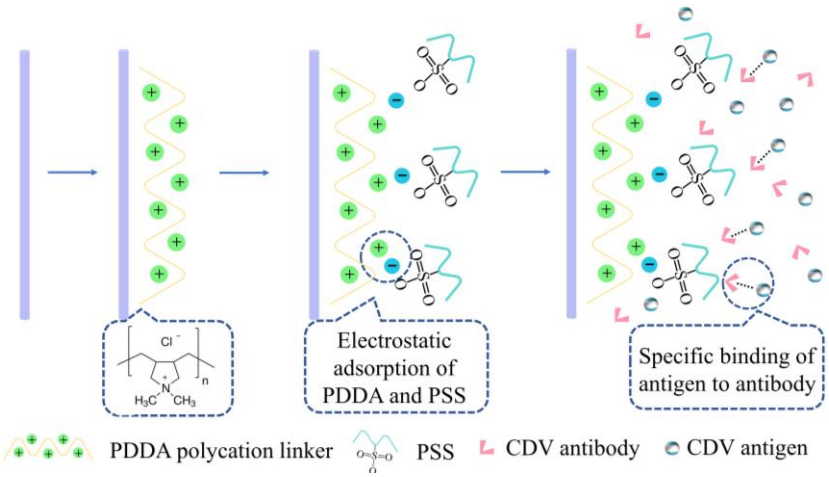

Fig. 3. Flow chart of fiber surface modification by decorating CDV antibody.

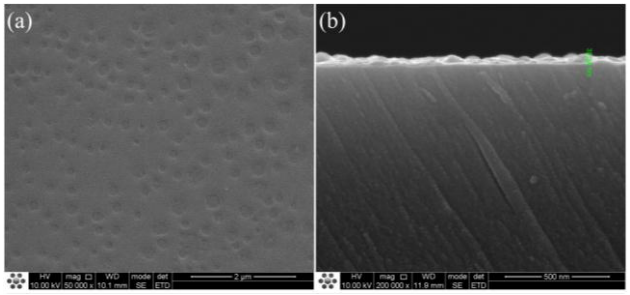

Fig. 4. SEM images of (a) fiber side, and (b) fiber cross-section.

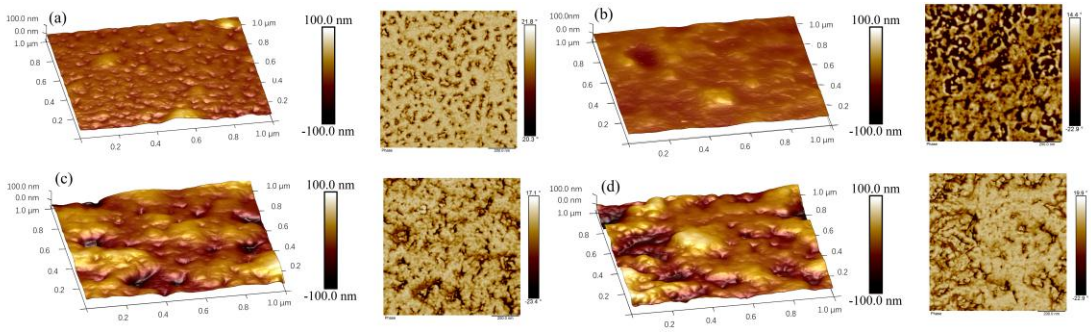

Fig. 5. AFM images: (a) surface topography of $(PDDA/PSS)_3$ multilayer films, (b) CDV antibody modification, (c) CDV antibody binding to 10 pg/ml antigen, and (d) CDV antibody binding to 10 ng/ml antigen.

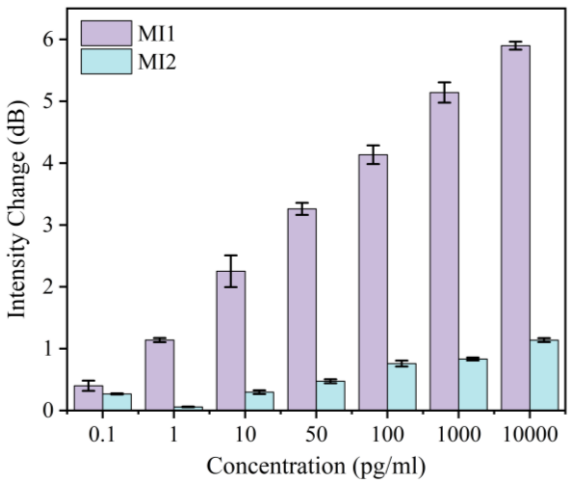

Fig. 6. MI1 and MI2 sensors to detect CDV antigens.

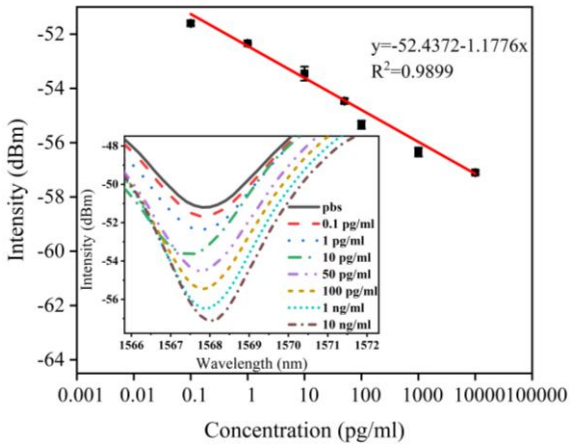

Fig. 7. Linear fitting of the trough near 1570 nm, illustrated with the response spectra at different concentrations of CDV antigen.

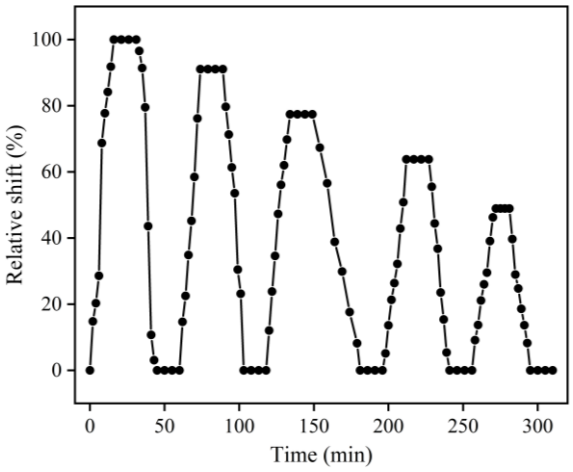

Fig. 8. Repeatability testing of CDV optic-fiber sensor.

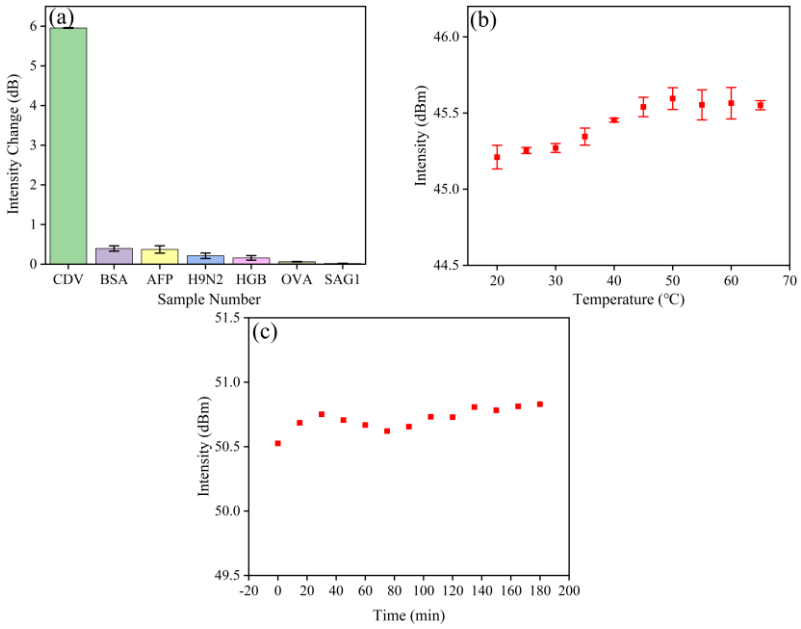

Fig. 9. (a) Selectivity, (b) temperature, and (c) time stability of the CDV optic-fiber sensor.

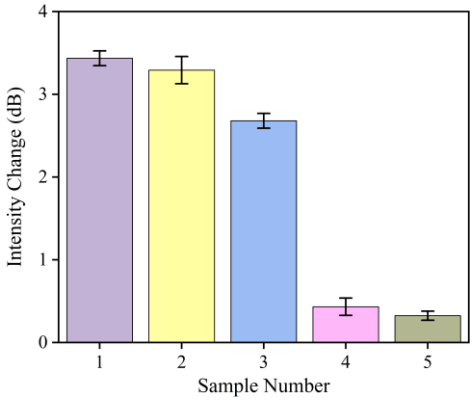

Fig. 10. Detection of clinical samples 1-3 are CDV active positive samples, and 4-5 are active negative samples.

Table 1 Comparison of different types of sensors

Detect Method	LOD (ng/ml)	Detection Range (ug/ml)	Sensitivity (dB/(pg/ml))	References
ELISA	0.8	--	--	[32]
Spot ELISA	0.2	--	--	[32]
Surface Plasmon Resonance	0.1	10^{2}-2.7×10^{4}	--	[33]
PCR	21	1.5×10^{-5}-1.5×10^{0}	--	[34]
Paper-based microfluidic immunoassay	6.35×10^{5}	--	--	[35]
Optic-fiber sensor	1.236×10^{-4}	10^{-7}-10^{-2}	1.1776	this work